Journal of Sound and Vibration (1983) **86**(4), 539–556

A SMALL STROUHAL NUMBER ANALYSIS FOR ACOUSTIC WAVE–JET FLOW–PIPE INTERACTION

S. W. RIENSTRA

National Aerospace Laboratory NLR, Amsterdam, The Netherlands

(*Received* 16 *January* 1982, *and in revised form* 9 *June* 1982)

Asymptotic expansions for small Strouhal number, valid for arbitrary subsonic Mach number, are derived for the solution of a simple problem of the interaction between an acoustic wave, a jet flow and a pipe, based on Munt's [1] exact formal solution. These expansions relate to the pressure and velocity fluctuations in the jet flow and in the far field, and to the reflection coefficient, end-impedance and end-correction for the reflected wave in the pipe. The field inside the flow is compared with experiments. The influence of a Kutta condition at the lip of the pipe is shown to be highly significant.

1. INTRODUCTION

Aerodynamic noise is usually an unwanted by-product of flow in technical applications. Of all the kinds, aircraft noise is probably most annoying, as it involves a great amount of acoustic energy and is produced in open air. A major aim of today's aircraft industries is therefore the reduction of this noise, and since jet noise has always been a main component of this aircraft noise, much research has been devoted to it. As a consequence, most of the general theoretical results in aeroacoustics have been tested only for the relatively complex situation of a jet flow, in which it is not always possible to isolate the specific theoretical aspect of interest. One can try to "clean up" the experiments, but even so it can still be difficult to decide whether the mechanism studied plays its imputed role or not. The other way to let experiments and theory meet each other is to refine the theoretical model to include elements which are important and inevitable in reality, although usually the model becomes as complicated as it is comprehensive. An example with typically this history is the study of the problem of the interaction of sound with a thin mixing layer, started by Miles [2] and Ribner [3] and culminating in Munt's [1] work.

Munt considered a semi-infinite circular thin-walled pipe from which issues into an inviscid medium a subsonic jet with "top hat" profile. Sound speed and mean density in and outside the jet may differ, while the ambient medium also flows in the same direction as, but more slowly than, the jet. The mixing layer is modelled by a cylindrical vortex sheet. The jet is perturbed by sound waves coming from inside the pipe. The possibility of instabilities is taken into account. The condition of smooth behaviour near the edge (Kutta condition) is applied (only possible if instabilities are included; see section 4). The problem is linearized according to the acoustic approximation. This model looks quite simple when compared with reality, particularly downstream in the jet, and it was not at all clear beforehand if convincing agreement with experiments would be obtained. A two dimensional variant of Munt's solution found by Crighton and Leppington [4] and Morgan [5] is difficult to test, while Savkar's [6] solution, only differing from Munt's in that no instabilities or Kutta condition are included, failed to give good agreement. However, Munt did find a remarkably good agreement for the far field directivity pattern [1] as well as for the open end reflection coefficient [7], and recently

0022-460X/83/040539+18 $03.00/0

Howe [8] showed that Munt's model includes essentially correctly the near field phenomenon of vortex shedding from the tube lip and its acoustic implications. Quoting Bechert [9]: "All results of this theory fit the available experimental data within the error band width of these experiments. This is quite an unusual situation in aeroacoustics".

This success provides a sufficient motive to proceed on the way indicated by Munt. Although the completeness of Munt's solution is just its power, this goes at the same time together with a complicated form, amenable only to a numerical evaluation. To provide some insight therefore, and with care taken to incorporate all the qualities of the exact solution, in the present paper, in a small Strouhal number asymptotic approximation, explicit analytical expressions are constructed *valid for all subsonic Mach numbers not close to unity*, with the aid of a method suggested by Boersma [10], to be explained below in section 4. With this low-frequency assumption all the modes of the sound in the tube are cut-off, except for the plane wave. A somewhat simpler version of Munt's problem is considered: i.e., no flowing ambient medium, and a uniform sound speed and mean density (cold jet). It is possible to relax this restriction. As reported elsewhere in more detail [11] the present method is also applicable when one has a slow ambient flow and sound speed and mean density ratios of order one (relative to the small Strouhal number). In the present paper, however, the concentration is on the basic physical processes and the necessary mathematical details of the method. Related calculations were carried out recently by Howe [8] and Cargill [12], concerning the modulus of the far field and the modulus of the reflection coefficient, with the Kutta condition applied. These solutions are not all systematically derived from Munt's exact solution, like ours, but they are, where comparable, in agreement with the present results.

More specifically the influence of application of the Kutta condition at the pipe lip is investigated, possible only when vortex shedding and instabilities are taken into account, by comparing the Kutta condition solution (Munt's solution) and the stable variant (in fact Savkar's [6] solution). (The acoustic singularity at the edge, viz. a pressure behaving like $1/r^{1/2}$ at the flow side, can be relieved by the shedding of vorticity; this vorticity triggers an instability if the mean flow is discontinuous across the edge streamline as is the case here. For one particular rate of vortex shedding the edge singularity is completely removed (Kutta condition) and turned into an $r^{1/2}$-behaviour.) The Kutta condition will be seen to be, at least in the lower Strouhal number range, crucial in Munt's solution, and cannot be ignored as was done by, e.g., Savkar [6], or Mungur and Plumblee [13].

A principal difficulty in Munt's analysis is how to select which instability of the jet is to be included, since sometimes (although not for the present case with small Strouhal number) more than only the cylindrical Helmholtz instability seem possible. These other, "secondary", modes [14, 15] are rapidly growing with an outgoing phase velocity but carrying a probably ingoing energy, and they are "physically unlikely", but a proper additional boundary condition to exclude them in the mathematical problem is not readily at hand. Munt found that application of a causality condition (to consider the source being activated at some time long ago) could resolve this issue, since then the Helmholtz instability remains as the only one possible. The author's view, however, is that this causality condition is physically not very well founded. This will be discussed in detail in section 2. Although no definite alternative will be given, the (for the moment) most relevant argument for the Helmholtz instability will be argued to be the analogy with the two-dimensional variant of the present problem, for which the solution is unambiguous without causality considerations.

In section 3 the problem is formulated, the formal exact solutions are given in section 4, the clue to the approximations is derived in section 5, and the expressions obtained for the field in the flow and the far field are constructed and discussed in section 6.

2. CAUSALITY AND KUTTA CONDITION

In this section the condition of causality, as introduced above, is considered in more detail. The definition of this causality is that the stationary field, as described by the mathematical model, viz. the differential equation and boundary conditions, is assumed to be started at some time long ago. So it is basically a *mathematical* boundary condition. Therefore, since one is, nevertheless, trying to model a *physical* problem, there is behind this causality condition the question of its physical relevance: i.e., whether it indeed relates to a physical mechanism whose absence from the model was responsible for a non-unique solution.

The absence of the start of the source itself is not to blame for being the most important missing aspect of the mathematical model.

Although in physical reality a time-harmonic behaviour can never be achieved for all time, the start of the source can always be put so far back in time that it is hidden by the inherent variety of small perturbations. So if this mathematical non-uniqueness reflects in any way the physics of the problem, it would have to come up from experiments as well. Yet, experiments are well reproducible [16, 17], and there is no evidence that the start of the source is important. What is really meant when introducing an argument of causality is that the source is considered to cause the field in the sense that the net energy propagates away from the source region. However, for the present model this cannot be determined yet and maybe never at all. In the simpler configuration of an acoustic field without mean flow or vortex shedding, it can be shown [18] that the above causality condition implies an outward energy flux, but this has still to be done for the present case, since no satisfactory definition for acoustic energy exists in a mean flow with vorticity [19]†. At the same time, it is not certain, at least in principle, whether an outward energy flux is always the correct condition, since the main flow may couple to the acoustic field, absorbing or supplying acoustic energy (both are possible [20]), and invalidating the principle of conserved energy. So if in a problem nothing is known of the sources of energy or the way the energy propagates, it is preferable, instead of using a causality condition, to try to extend the model by including viscosity, non-linearities, or a more detailed geometry, to obtain ultimately a model so close to reality that the solution is unambiguous. Although often the mathematical problem becomes untractable then, it is possible for a simpler version of the present problem to remove non-uniqueness difficulties by improving the modelling of the physical reality. At the same time this reveals so clearly the physical mechanism of the generation of the instability, that the author believes the same mechanism acts in this problem.

Consider a plane doubly infinite vortex sheet, separating a uniform subsonic flow from a stagnant flow, irradiated by a time harmonic line source, as studied by Jones and Morgan [21]. They found a non-unique solution with the Helmholtz instability as the eigensolution. By applying the above causality condition (of the source being switched on long ago), they could determine an amplitude of this instability uniquely. Later, the model was extended by Crighton and Leppington [4] and Morgan [5] to include a semi-infinite plate with trailing edge from which the vortex sheet develops. A set of causal solutions was found, only one of which satisfied the Kutta condition. However, causality was not necessary at all to determine the solution in a unique manner; the remaining unknown constant (the amplitude of the instability) is determined uniquely just by the edge condition (i.e., the Kutta condition). Any other boundary condition is superfluous [22]. Even more, it is more-or-less accidental that this Kutta condition

† Note: In the irrotational parts of the field, like the still medium or the uniform mean flow, an energy flux vector can be defined, and may inform us about some unacceptable sources. For instance, waves from sources at (irrotational parts of) infinity can be excluded.

solution is causal, since very easily non-causal, but still physically very acceptable, solutions can be constructed, if frequency dependent edge conditions are taken into consideration. So, when one assumes the edge condition to be most essential, causality is, in this case, not only superfluous, but might even conflict with the other boundary conditions.

In another way, the role of the edge dominates any effect of causality too. One could, in the Crighton and Leppington [4] problem, try to remove the plate away from the source region, to obtain a natural solution of the harmonic problem without plate. If causality is more essential than the edge condition, the Jones and Morgan [21] solution would result. This is, however, not the case. In fact, the field becomes singular everywhere [22]. The instability part tends to infinity like $\exp(kx_0(1+\mathrm{i})/M)y_s/x_0^{3/2}$ for plate position $-x_0 \to -\infty$, source position $(0, y_s)$ fixed and Mach number M small. (Apply Crighton and Leppington's small Mach number approximation to their equation (2.49).) The "distance attenuation" $(1/x_0^{1/2})$ and decreasing angle (y_s/x_0) is overshadowed by the exponential. (This is not implying that the Jones and Morgan solution is erroneous. What one actually has is a non-uniform double limit of plate edge and start of the source both going to infinity. The "Jones and Morgan instability" is a transient response, while the other develops from the edge.)

So one concludes that for the two-dimensional subsonic cold jet the problem of the Helmholtz instability generation is completely solved via the role of the edge condition. For a three-dimensional variant it is not fully solved, although one can argue, by analogy, that the (corresponding) Helmholtz instability is the only instability to be included, with an amplitude determined by the edge condition. But for problems with less in common, as for example the leading edge vortex generation studied recently by Goldstein [23], this analogy is speculative (see also the review paper of Crighton [24]).

For the present problem with a circular jet the matter is not discussed further, and the analogy with the two-dimensional problem is adopted.

3. FORMULATION OF THE PROBLEM

In an inviscid medium a subsonic uniform jet flow with velocity U_0 from a semi-infinite cylindrical rigid pipe with diameter D is perturbed by plane harmonic sound waves with frequency f^* coming from inside the pipe; see Figure 1. The fluid outside is at rest relative to the pipe. Mean density ρ_0, mean sound speed c_0 and mean pressure p_0 are equal inside and outside the flow. Beside viscosity, thermal conductivity and all non-linearities will also be ignored. The cylinder is specified by $r^* = \frac{1}{2}D$, $z^* \leqslant 0$ in cylindrical polar co-ordinates (r^*, θ, z^*), and the position of the undisturbed vortex layer, separating the jet from the ambient fluid, is given by $r^* = \frac{1}{2}D$, $z^* > 0$. One can introduce a potential ϕ^* for the velocity perturbations. The pressure perturbations are denoted by p^* and the perturbations in density by ρ^*. The time variable is t^*. The problem is made dimensionless

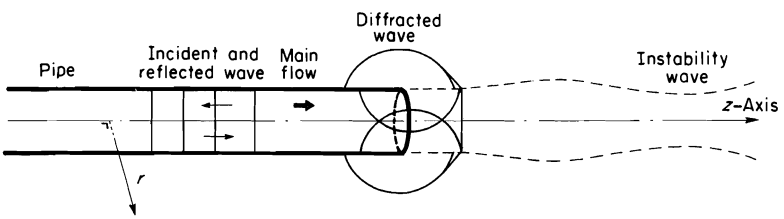

Figure 1. Sketch of the problem.

by introducing

$$\phi = \phi^*/\tfrac{1}{2}DU_0, \qquad r = r^*/\tfrac{1}{2}D, \qquad z = z^*/\tfrac{1}{2}D, \qquad t = t^*U_0/\tfrac{1}{2}D,$$
$$\omega = f^*\pi D/U_0, \qquad \rho = \rho^*/\rho_0, \qquad p = p^*/\rho_0 U_0^2.$$

The Mach number is $M = U_0/c_0$ (where $M < 1$), the Strouhal number is ω and the Helmholtz number is $k = \omega M = f^*\pi D/c_0$ (note the factor π difference from the usual definition). Finally, ω will be taken small to derive explicit expressions for axial velocity ϕ_z and pressure p inside the flow and pressure p outside in the far field from their respective exact analytic expressions in integral form. Munt's terminology is adopted with a few obvious simplifications. As usual, dependent variables are for convenience taken complex.

The primary wave ϕ_0, coming from inside the pipe, is given by

$$\phi_0(r, \theta, z, t) = a\phi_0(z)\exp(\mathrm{i}\omega t) = \begin{cases} a\mathrm{i}\dfrac{1+M}{\omega}\exp\left(-\mathrm{i}\dfrac{k}{1+M}z + \mathrm{i}\omega t\right), & r<1 \\ 0, & r>1 \end{cases}. \tag{3.1}$$

In this way the incident wave is normalized on pressure. The dimensionless amplitude a is taken small enough for linearization. As usual, the solution is assumed to have the same time and angle θ dependence as the primary wave. So here the solution is independent of θ, and dependent on time through the factor $\exp(\mathrm{i}\omega t)$; this factor, as well as the amplitude a, will be suppressed throughout. It is advantageous to write

$$\phi(r, z) = \phi_0(z) + \psi(r, z). \tag{3.2}$$

For convenience, to exclude incoming waves from infinity $r \to \infty$, the dimensionless wave number will be considered as a complex variable in a lower half of the complex plane. Therefore one writes

$$k = |k|\exp(-\mathrm{i}\delta) \quad \text{with } 0 < \delta < \pi. \tag{3.3}$$

Finally the limit $\delta \to 0$ will be taken.

The dimensionless position of the vortex sheet is given by

$$r = 1 + ah(z)\exp(\mathrm{i}\omega t), \qquad z > 0. \tag{3.4}$$

When the acoustic approximation $\rho = M^2 p$ is applied one obtains, with the above conventions, the following equations (indices z and r denote differentiation with respect to those variables):

$$\psi_{zz} + (1/r)(r\psi_r)_r + k^2\psi - 2\mathrm{i}kM\psi_z - M^2\psi_{zz} = 0, \qquad r<1, \tag{3.5}$$

$$\psi_{zz} + (1/r)(r\psi_r)_r + k^2\psi = 0, \qquad r>1, \tag{3.6}$$

$$p = -\mathrm{i}\{\omega/(1+M)\}\phi_0 - \mathrm{i}\omega\psi - \psi_z, \qquad r<1, \tag{3.7}$$

$$p = -\mathrm{i}\omega\psi, \qquad r>1. \tag{3.8}$$

The boundary conditions are as usual (where 1+, 1− mean upper, lower limit),

$$\psi_r(1, z) = 0, \quad z<0, \qquad p(1+, z) = p(1-, z), \quad z>0, \tag{3.9, 3.10}$$

$$\psi_r(1+, z) = \mathrm{i}\omega h(z), \quad z>0, \qquad \psi_r(1-, z) = \mathrm{i}\omega h(z) + h_z(z), \quad z>0, \tag{3.11, 3.12}$$

$$\psi(0, z) \text{ finite}. \tag{3.13}$$

The indices s and k will denote the stable and Kutta condition solution respectively.

The two edge conditions to be considered are in explicit form: for the Kutta condition that the pressure be finite, which is equivalent to assuming

$$h_k(z) = O(z^{3/2}) \qquad (z \downarrow 0), \tag{3.14}$$

while the condition for the stable solution is relaxed to allow the pressure to have an integrable singularity and uniqueness is assured by requiring the field to vanish at infinity. This is equivalent to

$$h_s(z) = O(z^{1/2}) \qquad (z \downarrow 0), \qquad h_s(z) \to 0 \qquad (z \to \infty). \tag{3.15}$$

4. EXACT SOLUTION

To obtain a causal solution (see section 2) Munt put first $\delta = \frac{1}{2}\pi$, constructed with spatial Fourier transforms and the Wiener–Hopf technique [25] a solution satisfying the Kutta condition, and found the physical solution afterwards via analytical continuation in k to real values of k (i.e., $\delta \to 0$). Also, without particular attention to causality properties of the solution, this is a convenient way to obtain with Fourier transformation the set of unstable solutions one is looking for here. What happens, when k is about imaginary, is that the Helmholtz instability is damped so much that the exponential growth is turned into a decay, giving a solution, Fourier transformable in the ordinary sense, which would otherwise be sifted out by a solution method based on Fourier transformation. Although the stable solution can be found the same way (but with another choice, i.e., zero, of the instability amplitude), the above argument indicates immediately a more simple approach, namely to leave δ near zero right from the start, and let the Fourier transformation sift out the only Fourier transformable solution, viz. the stable solution.

Details of the relevant calculations can be found in references [1] and [4], just the description of the solutions is sufficient here.

To start with one has δ small and positive. Then one can define the following half planes in the complex u plane,

$$R_+ = \{u \in \mathbb{C} \,|\, \mathrm{Im}\, u > \tan\delta\ (\mathrm{Re}\, u - (1+M)^{-1})\},\ R_- = \{u \in \mathbb{C} \,|\, \mathrm{Im}\, u < \tan\delta\ (\mathrm{Re}\, u + 1)\}, \tag{4.1, 4.2}$$

and the strip, common to R_+ and R_-,

$$S = \{u \in \mathbb{C} \,|\, -(1+M)^{-1} < \cot\delta\ \mathrm{Im}\, u - \mathrm{Re}\, u < 1\}. \tag{4.3}$$

The square roots

$$v_+(u) = (1-u)^{1/2}, \qquad v_-(u) = (1+u)^{1/2}, \tag{4.4, 4.5}$$

$$w_+(u) = \{1-(1+M)u\}^{1/2}, \qquad w_-(u) = \{1+(1-M)u\}^{1/2}, \tag{4.6, 4.7}$$

are defined as principal branches, i.e., $v_\pm(0) = w_\pm(0) = 1$, and the branch cuts run along the real axis to infinity, not crossing the origin. They define the functions

$$v = v_+ v_- \quad \text{and} \quad w = w_+ w_-, \tag{4.8}$$

in accord with the definition of Jones and Morgan [21] and Morgan [5], but not with that of Munt (Munt's v and w correspond to our w and v, respectively). The functions χ and μ, playing a central role, are defined as

$$\chi(-iku) = (1-uM)^2 v(u) \frac{\mathrm{J}_0(kw(u))}{\mathrm{J}_1(kw(u))} - w(u) \frac{\mathrm{H}_0^{(2)}(kv(u))}{\mathrm{H}_1^{(2)}(kv(u))} = (u-u_0)(u-u_1)\mu(u), \tag{4.9}$$

where J_n is the nth order Bessel function of the first kind, and $H_n^{(2)}$ the nth order Hankel function of the second kind [26]. The zeros and poles of χ are most important in the analysis. Of particular interest are the zeros u_0 and u_1, displayed separately. They are defined to correspond to the Helmholtz instability (u_0) and a related decreasing mode (u_1). They can be identified via their behaviour for $\omega \to i\infty$ and $M \to 0$ (then $u_0 = \bar{u}_1 \simeq (1+i)/M$), or for $\omega \to 0$ and $1-M^2 = O(1)$ (then $u_0 \simeq \bar{u}_1 \simeq M^{-1}\{1+i\frac{1}{2}\sqrt{2}\omega \ln^{1/2}\omega^{-1}\}$); the bar means complex conjugate. The function μ is related to Munt's $\hat{\mu}$ by $\mu(u) = -k^2\hat{\mu}(-iku)$. Note that in Munt's paper μ and u_1 have a different meaning. One can now introduce the split functions μ_+ and μ_-, regular and non-zero in the halfplanes R_+ and R_-, respectively, such that $\mu = \mu_+/\mu_-$. An auxiliary function $F_+(-iku)$ (in fact the Fourier transform of h, the vortex sheet displacement) is defined by

$$F_{+,k}(-iku) = A_0 N_+(u)(u-u_0)^{-1}, \qquad F_{+,s}(-iku) = A_0 N_+(u)\left(\frac{1}{1+M} - u_0\right)^{-1}, \tag{4.10, 4.11}$$

$$A_0 = -i\frac{1+M}{\omega^2} v_-\left(\frac{1}{1+M}\right) w_-\left(\frac{1}{1+M}\right) \mu_-\left(\frac{1}{1+M}\right), \qquad N_+(u) = \frac{v_+(u)}{w_+(u)\mu_+(u)(u-u_1)}.$$

Now one can formulate Munt's solution (for the present case). With δ taken to zero this is given by the following:

$r<1$:

$$\psi(r,z) = \frac{1}{2\pi i}\int_{-\infty-i\cdot 0}^{\infty+i\cdot 0} \frac{k(1-uM)F_+(-iku)J_0(kw(u)r)}{Mw(u)J_1(kw(u))} \exp(-ikuz)\,du - \left[\frac{k(1-u_0M)J_0(kw(u_0)r)\exp(-iku_0z)}{Mw(u_0)J_1(kw(u_0))}\{(u-u_0)F_+(-iku)\}_{u=u_0}\right]_k, \tag{4.12}$$

$r>1$:

$$\psi(r,z) = \frac{1}{2\pi i}\int_{-\infty-i\cdot 0}^{\infty+i\cdot 0} \frac{kF_+(-iku)H_0^{(2)}(kv(u)r)}{Mv(u)H_1^{(2)}(kv(u))} \exp(-ikuz)\,du - \left[\frac{kH_0^{(2)}(kv(u_0)r)\exp(-iku_0z)}{Mv(u_0)H_1^{(2)}(kv(u_0))}\{(u-u_0)F_+(-iku)\}_{u=u_0}\right]_k. \tag{4.13}$$

For small but finite δ the contour of integration runs through the strip S to infinity, as the Fourier transform of ψ is regular inside S. For $\delta \downarrow 0$ one has the contour then running just below the branch cuts along the negative real axis, just above the branch cuts along the positive real axis, and crossing the real axis somewhere between -1 and $(1+M)^{-1}$. In the expressions (4.12) and (4.13) the relevant F_+ is to be substituted from expression (4.10), or (4.11), according to the edge condition applied, while the expression between the brackets $[\ ]_k$ is to be added only in the case of the Kutta condition.

In the next section approximations for μ_+, μ_-, u_0 and u_1 will be calculated. In the subsequent section these will be used to evaluate pressure and axial velocity in the flow, and pressure in the far field. The reason that pressure and velocity inside the flow are both given is the following. In principle, the potential would be sufficient to describe the field, since all other flow variables can be obtained from it by differentiation. However, what one has here is only an approximation, and then differentiation is not always permitted. Indeed, in the region near the tube end two length scales for z are important, viz. the incident wave length and the pipe diameter, so differentiation with respect to z will decrease the relative order of magnitude of some terms; as a consequence, elements

of the error term of the potential may become relevant in the pressure or velocity. Although it is possible to retain in the potential certain terms to obtain a form which can stand differentiation, this form is complicated and not very well exploitable. It seems therefore most sensible to present pressure and velocity separately, with all the terms smaller than the error left aside, in the simplest form possible with the accuracy used.

5. APPROXIMATIONS FOR SMALL STROUHAL NUMBER OF THE FUNCTION χ

The central idea in the construction of the approximations is a method suggested to the author by Boersma [10]. It consists of a deformation of the contour of integration to a region wherein one can approximate the integrand uniformly. It will be applied for μ_+ and μ_-, and then in the same way for ψ. In fact two approximations for $\mu_\pm$ will be utilized: one inside the pipe and in the far field (the more accurate one), and the other one in the jet. The difference between these two is that the expression for ψ corresponding to the first approximation contains an exponentially large error downstream of the jet, which is avoided when using the alternative.

Introduce for convenience $\beta = (1-M^2)^{1/2}$. The only conditions on M are now expressed by $0<M<1$, and $\beta = O(1)$; M may be taken to zero, provided, of course, ω is kept small independently.

To start with, consider the contour of integration as introduced for ψ in expressions (4.12) and (4.13). Deform this contour by semi-circular indentations into R_+ around $u=1$ and $u=M^{-1}$ and into R_- around $u=-1$ (see Figure 2). The radii for $u=\pm 1$ are

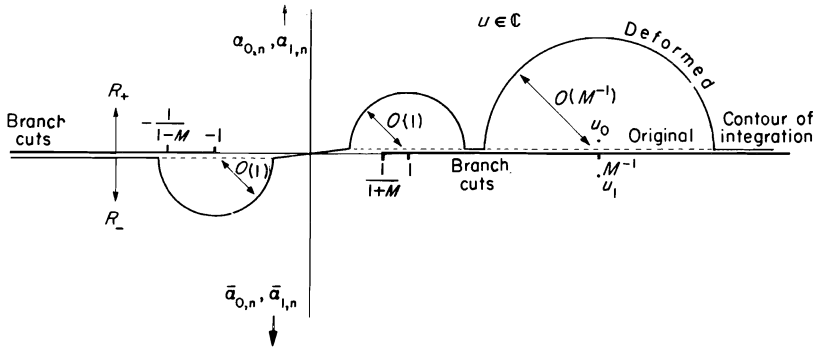

Figure 2. Zeros, poles and contours of integration in the complex u-plane.

$O(1)$ and smaller than 1, and for $u=M^{-1}$ are $O(M^{-1})$ and smaller than M^{-1} (so that on the new contour $v(u) \geqslant O(1)$ and $(1-uM)^2 \geqslant O(1)$). On this deformed contour χ may be approximated by

$$\tilde{x}(-\mathrm{i}ku) = (1-uM)^2 v(u)\, \mathrm{J}_0(kw(u))/\mathrm{J}_1(kw(u)), \tag{5.1}$$

with $\chi = \tilde{\chi}(1+O(\omega^2 \ln \omega^{-1}))$. This is seen by the following. First note that the relative error term is, for $|u| \leqslant 2/M$ on the new contour,

$$\left|\frac{\mathrm{H}_0^{(2)}(kv(u))\mathrm{J}_1(kw(u))w(u)}{\mathrm{H}_1^{(2)}(kv(u))\mathrm{J}_0(kw(u))v(u)(1-uM)^2}\right| \approx \left|\frac{1}{2}\frac{k^2 w^2(u)}{(1-uM)^2}\ln(kv(u))\right| = O(\omega^2 \ln \omega^{-1}). \tag{5.2}$$

For larger $|u|$ on the contour v and w are negative purely imaginary, so that

$$|\text{rel. err.}| = \mathrm{K}_0(k|v|)\mathrm{I}_1(k|w|)|w|/\mathrm{K}_1(k|v|)\mathrm{I}_0(k|w|)|v|(1-uM)^2,$$

where I_n and K_n are modified Bessel functions of the 1st and 2nd kind. For small $k|v|$ and $k|w|$ one can use the same approximation as for $|u| \leqslant 2/M$, so then the relative error is $O(\omega^2 \ln \omega^{-1})$. One knows [26] that I_n and K_n have no positive real zeros or singularities and furthermore have the behaviour $K_0/K_1 \to 1$, $I_1/I_0 \to 1$ for $k|u| \to \infty$, so for $k|v|$ and $k|w| \geqslant O(1)$ the relative error is $O((uM)^{-2}) \leqslant O(\omega^2) < O(\omega^2 \ln \omega^{-1})$.

With some algebra one can find the following approximations for the zeros u_0 and u_1:

$$\tilde{u}_0 = M^{-1}(1 + i\omega\sqrt{L}), \qquad \tilde{u}_1 = M^{-1}(1 - i\omega\sqrt{L - \tfrac{1}{2}\pi i}), \tag{5.3}$$

with $L = -\frac{1}{2}\ln(\frac{1}{2}\omega\beta\, e^{\gamma})$, $\gamma = 0{\cdot}5772\ldots$ Euler's constant, the principal branch for the square root and $u_{0,1} = \tilde{u}_{0,1}(1 + O(\omega^2 \ln \omega^{-1}))$. Now one has on the deformed contour $u - u_{0,1} = (u - \tilde{u}_{0,1})\,(1 + O(\omega^2 \ln \omega^{-1}))$. The zero $u = M^{-1}$ of $\tilde{\chi}$ corresponds to the zeros u_0 and u_1 of χ, but is not a sufficiently good approximation for $u_{0,1}$ to retain the accuracy used so far, as is seen from expressions (5.3). Therefore one needs

$$\tilde{\mu}(u) = (1 - uM)^2 v(u) J_0(kw(u))/(u - \tilde{u}_0)(u - \tilde{u}_1) J_1(kw(u)) \tag{5.4}$$

to approximate μ on the new contour with $\mu = \tilde{\mu}(1 + O(\omega^2 \ln \omega^{-1}))$. With the infinite product decompositions [26]

$$J_0(z) = \prod_{n=1}^{\infty} (1 - (z/j_{0,n})^2), \qquad J_1(z) = \tfrac{1}{2}z \prod_{n=1}^{\infty} (1 - (z/j_{1,n})^2)$$

(with $j_{0,n}$, $j_{1,n}$ the nth zero of J_0, J_1), one can construct from $\tilde{\mu}$ approximations $\tilde{\mu}_{\pm}$ for the split functions $\mu_{\pm}$, viz.

$$\tilde{\mu}_+(u) = \frac{(u - M^{-1})^2}{(u - \tilde{u}_0)(u - \tilde{u}_1)} \frac{v_+(u)}{w_+(u)} \prod_{n=1}^{\infty} \frac{(u - \bar{\alpha}_{0,n}) j_{1,n}}{(u - \bar{\alpha}_{1,n}) j_{0,n}}, \tag{5.5}$$

$$\tilde{\mu}_-(u) = \tfrac{1}{2}kM^{-2} \frac{w_-(u)}{v_-(u)} \prod_{n=1}^{\infty} \frac{(u - \alpha_{1,n}) j_{0,n}}{(u - \alpha_{0,n}) j_{1,n}}, \tag{5.6}$$

where $\alpha_{m,n} = i(\beta k)^{-1}\{j_{m,n}^2 - (k/\beta)^2\}^{1/2} - M\beta^{-2}$, the bar means complex conjugate, and the accuracy is $\mu_{\pm} = \tilde{\mu}_{\pm}(1 + O(\omega^2 \ln \omega^{-1}))$ on the deformed contour. This relative accuracy and the fact that $\tilde{\mu}_+$ is singular at $u = \tilde{u}_0$, which is an element of R_+, may not be obvious, but can be seen by the following arguments. One can call, for definiteness, the deformed contour of the above the "deformed ψ-contour".

As is well known one can express μ_+ and μ_- exactly by the formal representation (modulo an integral non-zero function) [25, p. 16]

$$\ln \mu_{\pm}(u) = \frac{1}{2\pi i} \int_{-\infty - i\cdot 0}^{\infty + i\cdot 0} \frac{\ln \mu(u')}{u' - u}\, du', \tag{5.7}$$

where for μ_+ one must have $u \in R_+$ above the integration contour, and for $\mu_- u \in R_-$ below the contour. For "opposite" values, i.e., $u \in R_{\mp}$ for $\mu_{\pm}$, one uses the identity $\mu_+ = \mu\mu_-$. The integration contour for μ_+ runs just below and for μ_- just above that for ψ in equations (4.12) and (4.13), although in the same way with respect to the branch cuts. If the integral of equation (5.7) does not converge, this can be cured but is not important here. Now deform the μ_+-contour in the same way as before for ψ (Figure 2), so that the deformed μ_+-contour is everywhere close to and just below the deformed ψ-contour. Between the deformed and the old contour $\ln \mu(u')$ is an analytic function. (Branch cuts of v and w run along the real axis, while for $|u'| \leqslant 2/M$ is $\chi \simeq (1 - u'M)^2 v/(kw) + kvw \ln(kv)$, the only relevant zero of which is divided out in $\mu(u')$ as the factor $u' - u_0$.) So for $u \in R_+$ above the new μ_+-contour (in particular for u on

the deformed ψ-contour) the integral of equation (5.7) is the same for the old and the new contour. On this new contour $\tilde{\mu}$ approximates μ, and therefore one can write, with some mild additional assumptions concerning the error term,

$$\ln \mu_+(u) = \frac{1}{2\pi i} \oint_{-\infty-i\cdot 0}^{\infty+i\cdot 0} \frac{\ln \mu(u')}{u'-u}\,du' = \frac{1}{2\pi i} \oint_{-\infty-i\cdot 0}^{\infty+i\cdot 0} \frac{\ln \tilde{\mu}(u')}{u'-u} + O(\omega^2 \ln \omega^{-1}),$$

where the sign $\subset$ means a deformed contour according to Figure 2. Evaluation of the final integral (close the contour via the upper half u-plane), an analogous procedure for μ_- in R_- and using $\mu_+ = \mu\mu_-$ yield the expressions (5.5) and (5.6). It is evident from the above that also $\mu_-((1+M)^{-1}) = \tilde{\mu}_-((1+M)^{-1})(1+O(\omega^2 \ln \omega^{-1}))$. For the far field one needs the value $\mu_+(\cos\xi)$ with ξ some real number with $0<\xi<\pi$. If one assumes the restriction that there is a positive number n of order 1 with $\xi \geqslant O(\omega^n)$, then also for this case one can use the present approximation, and one has, for all M, $\mu_+(\cos\xi) = \tilde{\mu}_+(\cos\xi)(1+O(\omega^2 \ln \omega^{-1}))$. This is seen with the following. Whenever $0<(1+M)^{-1} - \cos\xi = O(1)$ the deformed μ_+-contour can be kept below $u' = \cos\xi$ and the result follows at once. When $(1+M)^{-1} - \cos\xi$ is small or negative, the μ_+-contour crosses the pole $u' = \cos\xi$ of expression (5.7) with deformation and one obtains first $\mu_+(\cos\xi) = \mu(\cos\xi)\tilde{\mu}_-(\cos\xi)(1+O(\omega^2 \ln \omega^{-1}))$. Then the required result follows from the fact that still $\mu(\cos\xi) = \tilde{\mu}(\cos\xi)(1+O(\omega^2 \ln \omega^{-1}))$, since one has $\mu(\cos\xi) = \chi(-ik\cos\xi) \cdot (\cos\xi - \tilde{u}_0)^{-1}$ $(\cos\xi - \tilde{u}_1)^{-1}(1+O(\omega^2 \ln \omega^{-1}))$, while furthermore $\chi(-ik\cos\xi) \simeq \tilde{\chi}(-ik\cos\xi)$ with a relative error, given by expression (5.2), which is $|\frac{1}{2}k^2 w^2(\cos\xi)(1-M\cos\xi)^{-2} \ln(k\sin\xi)| \leqslant O(\omega^2 \ln \omega^{-1})$ because $\xi \geqslant O(\omega^n)$.

The approximations are now to be substituted into the integral formulations for ψ, and, via the same contour deformation as for $\tilde{\mu}$, one can evaluate an approximation to ψ. However, an accurate approximation for μ does not automatically lead to an accurately approximated ψ. Far upstream and far downstream the flow the expression for ψ consists mainly of the contributions from residues of the poles $u = -(1-M)^{-1}$, $(1+M)^{-1}$, u_0 and u_1, (among other things) through a factor $\exp(-ikuz)$. This implies that a shift of the imaginary part of these poles induces an exponentially large error in ψ for increasing $|z|$. For the present approximation the poles $u = -(1-M)^{-1}$ and $(1+M)^{-1}$ are not approximated, so upstream one will meet no such difficulty, but downstream the shift of the poles $u = u_0$ and u_1 to M^{-1} will obviously limit the validity of the solution there. Therefore an effort has been made to find an alternative approximation to μ to remedy this shortcoming. This was indeed possible (see below), but at the expense of a larger relative error, viz. $O(\omega \ln^{-1/2} \omega^{-1})$ instead of $O(\omega^2 \ln \omega^{-1})$. So this new one is not usefully applied everywhere. One can therefore use the above approximation where possible (upstream inside the pipe, and in the far field outside the instability region) and the other one (to be presented below) in the jet. Inside the instability cone the far field will not be considered, being a poor representation of reality anyway.

The alternative approximations to μ_+ and μ_- are as follows. The lines of argument are the same as for $\tilde{\mu}_\pm$ above so only the results are presented. The zeros u_0 and u_1 are now assumed to be known exactly:

$$\chi(-iku) \simeq M^2(u-u_0)(u-u_1)v(u)\frac{J_0(kw(u))}{J_1(kw(u))}, \tag{5.8}$$

$$\mu(u) \simeq M^2 v(u)\frac{J_0(kw(u))}{J_1(kw(u))}, \qquad \mu_+(u) \simeq \frac{v_+(u)}{w_+(u)} \prod_{n=1}^{\infty} \frac{(u-\bar{\alpha}_{0,n})j_{1,n}}{(u-\bar{\alpha}_{1,n})j_{0,n}}, \tag{5.9, 5.10}$$

all with a relative accuracy of $O(\omega \ln^{-1/2}\omega^{-1})$. The approximation to μ_- turns out to be identical to $\tilde{\mu}_-$ of expression (5.6). It is to be noted that in reference [11] this second

approximation is not included, and, consequently, the region of validity of the solution downstream had to be limited.

One is now ready to evaluate the approximations of the physical variables under consideration. For the field inside the flow one follows the same procedure as above for μ. The contour ψ is deformed (Figure 2) to open the possibility of applying the approximations of $\mu_\pm$ and of $u-u_{0,1}$; the crossing of the pole $u=u_0$ must be taken into account in the case of the unstable (Kutta condition) solution. The far field is obtained by direct substitution of the present approximations for $\mu_\pm$ and $u_{0,1}$ into the stationary phase far field approximation for ψ.

6. THE FIELD INSIDE THE FLOW AND THE FAR FIELD

The evaluation of the integrals obtained is standard and need not be mentioned here. One finds

$$p_s(r, z\geqslant 0)=\frac{2M}{1-M}\Sigma_0'\left(r,\frac{z}{\beta}\right)\exp\left[\frac{\mathrm{i}kM}{\beta^2}z-\mathrm{i}\omega(1+M)\sqrt{L}-\frac{\mathrm{i}k}{\beta}C_J\right]+\frac{2\mathrm{i}k}{(1-M)\beta}\Sigma_0\left(r,\frac{z}{\beta}\right)$$
$$+O(\omega\ln^{-1/2}\omega^{-1}), \tag{6.1}$$

$$p_s(r, z\leqslant 0)=\exp\left[-\frac{\mathrm{i}k}{1+M}z\right]-\frac{1+M}{1-M}\exp\left[\frac{\mathrm{i}k}{1-M}z-2\mathrm{i}k\sqrt{L}-2\frac{\mathrm{i}k}{\beta}C_J\right]$$
$$+\frac{2M}{1-M}\Sigma_1'\left(r,\frac{z}{\beta}\right)\exp\left[\frac{\mathrm{i}kM}{\beta^2}z-\mathrm{i}\omega(1+M)\sqrt{L}-\frac{\mathrm{i}k}{\beta}C_J\right]+\frac{2\mathrm{i}k}{(1-M)\beta}\Sigma_1\left(r,\frac{z}{\beta}\right)$$
$$+O(\omega^2\ln\omega^{-1}), \tag{6.2}$$

$$\frac{\partial}{\partial z}\phi_s(r, z\geqslant 0)=2\mathrm{i}k(1+M)\sqrt{L-\tfrac{1}{2}\pi\mathrm{i}}\exp(-\mathrm{i}ku_1z)$$
$$-\frac{2M}{1-M}\Sigma_0'\left(r,\frac{z}{\beta}\right)\exp\left[\frac{\mathrm{i}kM}{\beta^2}z-\mathrm{i}\omega(1+M)\sqrt{L}-\frac{\mathrm{i}k}{\beta}C_J\right]$$
$$-\frac{2\mathrm{i}kM^2}{(1-M)\beta}\Sigma_0\left(r,\frac{z}{\beta}\right)+O(k\ln^{-1/2}\omega^{-1}), \tag{6.3}$$

$$\frac{\partial}{\partial z}\phi_s(r, z\leqslant 0)=M\exp\left[-\frac{\mathrm{i}k}{1+M}z\right]+\frac{1+M}{1-M}M\exp\left[\frac{\mathrm{i}k}{1-M}z-2\mathrm{i}k\sqrt{L}-2\frac{\mathrm{i}k}{\beta}C_J\right]$$
$$-\frac{2M}{1-M}\Sigma_1'\left(r,\frac{z}{\beta}\right)\exp\left[\frac{\mathrm{i}kM}{\beta^2}z-\mathrm{i}\omega(1+M)\sqrt{L}-\frac{\mathrm{i}k}{\beta}C_J\right]$$
$$-\frac{2\mathrm{i}kM^2}{(1-M)\beta}\Sigma_1\left(r,\frac{z}{\beta}\right)+O(k\omega\ln\omega^{-1}), \tag{6.4}$$

$$p_k(r, z\geqslant 0)=\frac{2}{M^2(u_0-u_1)}\exp\left[-\mathrm{i}kC_J\left(\frac{1-M}{1+M}\right)^{1/2}\right]\cdot\left\{\frac{(1-u_0M)^2}{w^2(u_0)}\exp\left[-\mathrm{i}ku_0(z-\beta C_J)\right]\right.$$
$$\left.-\frac{(1-u_1M)^2}{w^2(u_1)}\exp\left[-\mathrm{i}ku_1(z-\beta C_J)\right]\right\}+\frac{2\mathrm{i}k}{\beta}\Sigma_0\left(r,\frac{z}{\beta}\right)$$
$$+\text{rel. err. }O(\omega\ln^{-1/2}\omega^{-1}), \tag{6.5}$$

$$p_k(r, z \leqslant 0) = \exp\left[-\frac{ik}{1+M} z\right] - \exp\left[\frac{ik}{1-M} z - 2\frac{ik}{\beta} C_J\right] + \frac{2ik}{\beta} \Sigma_1\left(r, \frac{z}{\beta}\right) + O(\omega^2 \ln \omega^{-1}), \tag{6.6}$$

$$\frac{\partial}{\partial z} \phi_k(r, z \geqslant 0) = \frac{2}{M(u_0 - u_1)} \exp\left[-ikC_J\left(\frac{1-M}{1+M}\right)^{1/2}\right] \left\{\frac{u_0(1-u_0M)}{w^2(u_0)} \exp\left[-iku_0(z-\beta C_J)\right]\right.$$
$$\left. - \frac{u_1(1-u_1M)}{w^2(u_1)} \exp\left[-iku_1(z-\beta C_J)\right]\right\} - \frac{2ik}{\beta} \Sigma_0\left(r, \frac{z}{\beta}\right)$$
$$+ \text{rel. err. } O(\omega \ln^{-1/2} \omega^{-1}), \tag{6.7}$$

$$\frac{\partial}{\partial z} \phi_k(r, z \leqslant 0) = M \exp\left[-\frac{ik}{1+M} z\right] + M \exp\left[\frac{ik}{1-M} z - 2\frac{ik}{\beta} C_J\right] - \frac{2ik}{\beta} \Sigma_1\left(r, \frac{z}{\beta}\right)$$
$$+ O(k\omega \ln \omega^{-1}). \tag{6.8}$$

Representations of the constant C_J are

$$C_J = 0{\cdot}25537\ldots = \sum_{n=1}^{\infty} \left(\frac{1}{j_{0,n}} - \frac{1}{j_{1,n}}\right) = \Sigma_0(0, 0) - \Sigma_1(0, 0) = \int_0^{\infty} \ln\left[\tfrac{1}{2} x I_0(x)/I_1(x)\right] \frac{dx}{\pi x^2}. \tag{6.9}$$

The functions Σ_0 and Σ_1 are defined by

$$\Sigma_0(r, z') = \sum_{m=1}^{\infty} \frac{J_0(rj_{0,m}) \exp(-z' j_{0,m})}{j_{0,m}(1 + j_{0,m}/j_{1,m}) \prod_{\substack{n=1 \\ n \neq m}}^{\infty} (1 - j_{0,m}/j_{0,n})(1 + j_{0,m}/j_{1,n})}$$

$$\approx 0{\cdot}3774 - 0{\cdot}66z' + \cdots \quad \text{for } z' \to 0, r = 0, \tag{6.10}$$

$$\Sigma_1(r, z') = \sum_{m=1}^{\infty} \frac{J_0(rj_{1,m}) \exp(z' j_{1,m})}{j_{1,m}(1 + j_{1,m}/j_{0,m}) \prod_{\substack{n=1 \\ n \neq m}}^{\infty} (1 + j_{1,m}/j_{0,n})(1 - j_{1,m}/j_{1,n})}, \tag{6.11}$$

while $\Sigma'_{0,1}(r, z') \equiv (\partial/\partial z') \Sigma_{0,1}(r, z')$. Furthermore, it may be noted that, for any $r < 1$, $\Sigma_0(r, z')$ and $\Sigma_1(r, z') - z' + C_J$ represent the same function analytic in z'.

It is interesting to observe that the rather crude approximations

$$j_{0,n} \approx (n - \tfrac{1}{4})\pi, \qquad j_{1,n} \approx (n + \tfrac{1}{4})\pi, \tag{6.12}$$

only correct for large n, give the promising result $C_J \approx 4\pi^{-1} - 1 = 0{\cdot}2732\ldots$, which is only 7% in error. It may therefore be useful, to obtain explicit figures with the least numerical effort, to apply this approximation (6.12) in Σ_0 and Σ_1. On the pipe axis $r = 0$ one can express the derivatives Σ'_0 and Σ'_1 then entirely in elementary functions, and Σ_0 and Σ_1 nearly entirely. After some algebra one finds

$$\hat{\Sigma}_0(0, z') = -\frac{8\sqrt{2}}{\pi^2} \int_0^{\exp(-\frac{1}{4}\pi z')} \frac{t^2 \ln t}{1 + t^4} dt$$
$$+ \frac{2}{\pi^2}(1 - \tfrac{1}{4}\pi z') \left[\pi + \ln \frac{2\cosh(\tfrac{1}{4}\pi z') - \sqrt{2}}{2\cosh(\tfrac{1}{4}\pi z') + \sqrt{2}} - 2 \arctan\{\sqrt{2} \sinh(\tfrac{1}{4}\pi z')\}\right]$$
$$= 0{\cdot}3897 - 0{\cdot}6696z' + O(z'^2) \quad \text{for } z' \to 0, \tag{6.13}$$

$$\hat{\Sigma}_1(0, z') = \hat{\Sigma}_0(0, z') + z' + 1 - 4/\pi. \tag{6.14}$$

Use is made of the identity

$$\prod_{\substack{n=1\\ n\neq m}}^{\infty}\left(1-\frac{m-\frac{1}{4}}{n-\frac{1}{4}}\right)\left(1+\frac{m-\frac{1}{4}}{n+\frac{1}{4}}\right)=-\tfrac{1}{8}\sqrt{2}\pi(-1)^m(1-(4m)^{-2}).$$

In Figure 3, these $\hat{\Sigma}_{0,1}$, together with the original $\Sigma_{0,1}$, are plotted on a logarithmic scale. The accuracy of $\hat{\Sigma}_{0,1}$, as approximating $\Sigma_{0,1}$, is seen to be quite good.

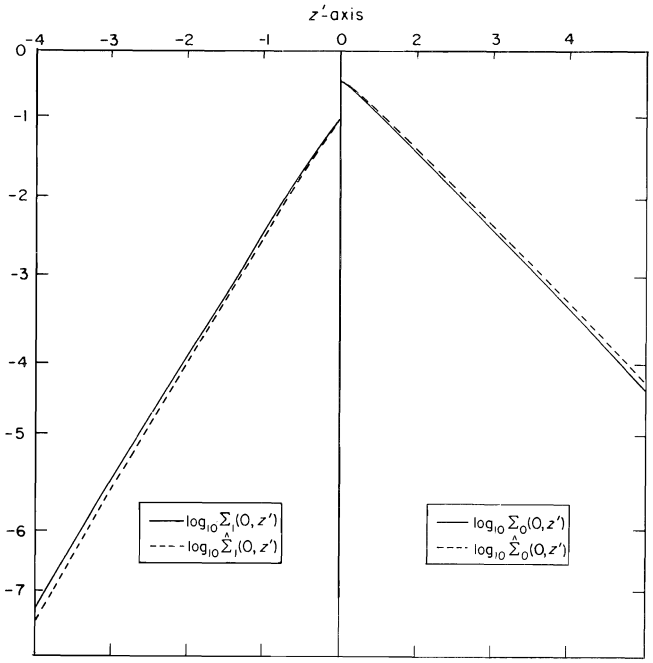

Figure 3. The auxiliary functions $\Sigma_0(0, z')$ $(z'>0)$ and $\Sigma_1(0, z')$ $(z'<0)$ (6.10) and (6.11), and their approximations $\hat{\Sigma}_0(0, z')$ and $\hat{\Sigma}_1(0, z')$ (6.13) and (6.14).

The expressions (6.1), (6.3), (6.5) and (6.7) with expression (5.3) show that (except far downstream) the instability waves are absent from the pressure and consist purely of a convected vorticity pattern. More physical information provided by the expressions (6.1)–(6.8) is given by the following quantities:
the impedance at $z=0$: $Z=Z^*/\rho_0 c_0=Mp(r, 0)/\phi_z(r, 0)$,

$$Z_s=-M-\frac{ik\beta}{\Sigma_0'(r, 0)}\left[\beta\sqrt{L}+\Sigma_0(r, 0)\right]+O(\omega^2\ln\omega^{-1}), \tag{6.15}$$

$$Z_k=\frac{ik}{\beta}\Sigma_0(r, 0)+O(\omega^2\ln\omega^{-1}); \tag{6.16}$$

the reflection coefficient R for pressure: quotient of the complex amplitudes of reflected and primary wave,

$$R_s=-\frac{1+M}{1-M}\exp\left[-2ik\sqrt{L}-2\frac{ik}{\beta}C_J\right]+O(\omega^2\ln\omega^{-1}), \tag{6.17}$$

$$R_k=-\exp\left[-2\frac{ik}{\beta}C_J\right]+O(\omega^2\ln\omega^{-1}); \tag{6.18}$$

the end correction l: point $l = z \bmod \pi\beta^2/k$ where primary and reflected pressure waves are 180° out of phase,

$$l_s = \beta^2\sqrt{L} + \beta C_J + O(\omega M^{-1} \ln \omega^{-1}), \qquad l_k = \beta C_J + O(\omega M^{-1} \ln \omega^{-1}). \quad (6.19, 6.20)$$

Observe that "basic" variables such as pressure and velocity are approximated uniformly in M; this is not always true of such "secondary" quantities as the end correction.

These impedances, reflection coefficients and end corrections in expressions (6.15)–(6.20) show how sensitive the solution is in (at least) the small Strouhal number range to the edge condition. One can conclude that, if possible, experimental data should include in some way information concerning the actual edge behaviour. It is otherwise virtually impossible to verify analytical calculations of the present type experimentally. Of course, on the other hand, as soon as experiments have confirmed the present results in sufficient detail, the results can be used to estimate in future experiments what the edge behaviour must be.

It is fascinating to see that the non-uniform behaviour of the limit $(k, M) \to (0, 0)$ in the hydrodynamic sense corresponds to non-uniform behaviour also acoustically. For $k \to 0$ with $\omega \to \infty$ ($M \ll k$, without vortex shedding) one obtains the no-flow case to which is associated an end correction of $l_0 = 0{\cdot}6133\ldots$ [27]; for $k \to 0$ with $\omega \to 0$ ($k \ll M$) sufficiently fast one has a case of incompressible flow with an end correction depending on the edge condition: $l = C_J = 0{\cdot}2554$ (Kutta), $l = \sqrt{L}$ (stable), etc. This non-uniform behaviour could be observed already in χ of expression (4.9). For $M = 0$ and finite k the factor $(1 - uM)^2$ becomes unity and consequently for large $|u|$ $\tilde{\chi}$ of expression (5.1) does not approximate χ any more.

The present approximations for $\mu_\pm$ and $u_{0,1}$ are also applicable to the far field expressions, and give in a very straightforward way useful results. This is discussed briefly in what follows. A further analogous treatment of the far field has been given by Cargill [12].

Define $r = \bar{r} \sin \xi$, $z = \bar{r} \cos \xi$ with $0 < \xi < \pi$. "Far field" here means the leading order term in the asymptotic evaluation for $k\bar{r} \to \infty$. The error term will implicitly be understood and will not be mentioned. One knows from Munt [1] that the method of stationary phase provides the following result. Not close to $\xi = \pi$ (to stay outside the pipe), and sufficiently far from $\xi = 0$ (i.e., not close to $\xi = 0$ to stay outside the flow for the stable case, and $\cos \xi < \frac{1}{2}\sqrt{2}[1 + |u_0|^2 - \{(|u_0|^2 - 1)^2 + 4\,(\mathrm{Im}\, u_0)^2\}^{1/2}]^{1/2}$ for any unstable case to stay away from the instability wave which does not represent reality very well far downstream), the far field is given by

$$p(\bar{r}, \xi) \approx -\frac{\mathrm{i}\omega^2}{\pi \sin \xi} \cdot \frac{F_+(-\mathrm{i}k \cos \xi)}{\mathrm{H}_1^{(2)}(k \sin \xi)} \frac{\exp(-\mathrm{i}k\bar{r})}{k\bar{r}}. \quad (6.21)$$

For small ω (and hence small $k = \omega M$) this becomes, (with expressions (5.3), (5.5) and (5.6) and the discussion in the middle of section 5, for $\xi \geqslant \omega\sqrt{L}/\beta$ in the Kutta condition case and for $\xi \geqslant O(\omega^n)$ for some $n = O(1)$ in the stable case),

$$\begin{aligned} p_s(\bar{r}, \xi) \approx {} & \tfrac{1}{2}\mathrm{i}k^2(1+M) \frac{\exp(-\mathrm{i}k\bar{r})}{k\bar{r}} \frac{1 - M\cos\xi + \mathrm{i}\omega\sqrt{L}}{(1 - M\cos\xi)^2} \\ & \times \exp\left[-\mathrm{i}\omega(1+M)\sqrt{L} - \mathrm{i}k\left(\frac{1-M}{1+M}\right)^{1/2} C_J + \mathrm{i}k\beta C_J \cos\xi\right] \\ & \times (1 + O(\omega^2 \ln \omega^{-1})), \end{aligned} \quad (6.22)$$

$$p_k(\bar{r},\xi) \approx \tfrac{1}{2}ik^2 \frac{\exp(-ik\bar{r})}{k\bar{r}} \frac{1}{(1-M\cos\xi)^2} \exp\left[-ik\left(\frac{1-M}{1+M}\right)^{1/2} C_J + ik\beta C_J \cos\xi\right]$$
$$\times (1+O(\omega^2 \ln \omega^{-1})). \tag{6.23}$$

The intensity of the free space radiation [19, p. 43] is then $\bar{I}^* = \rho_0 U_0^3 \bar{I} = \frac{1}{2}\rho_0 U_0^3 M|p|^2$,

$$\bar{I}_s = \frac{k^2 M}{8\bar{r}^2} \frac{(1+M)^2}{(1-M\cos\xi)^2} (1+O(\omega^2 \ln \omega^{-1})), \tag{6.24}$$

$$\bar{I}_k = \frac{k^2 M}{8\bar{r}^2} \frac{1}{(1-M\cos\xi)^4} (1+O(\omega^2 \ln \omega^{-1})). \tag{6.25}$$

The difference between these two is clearly a factor $(1+M)^{-2}$ and a squared Doppler factor, associated with the convected vortices, which provide, especially for high Mach number, a significantly different directivity.

It has been shown by Cargill [12] that expression (6.25) agrees remarkably well with Munt's numerical results and with experiments even for ω up to two.

A comparison of the field in the flow is given in Figures 4 and 5. The corresponding values of u_0 and u_1 are given in Table 1. In Figure 4, the Kutta condition pressure field (6.5) and (6.6), and the stable variant (6.1) and (6.2), are plotted together with experimental data obtained by Moore ([16], Figure 20). Inside the pipe the experimental and theoretical maxima are matched to determine the amplitudes. For esthetic reasons (the error is basically the same) the downstream part of the solution is matched at the pipe exit to the upstream part to remove the discontinuity at $z = 0$, which is inherent to the approximate character of the solution. Even though the occurring Strouhal numbers are not really small (they vary from 0·56 to 1·12), the agreement of the Kutta condition

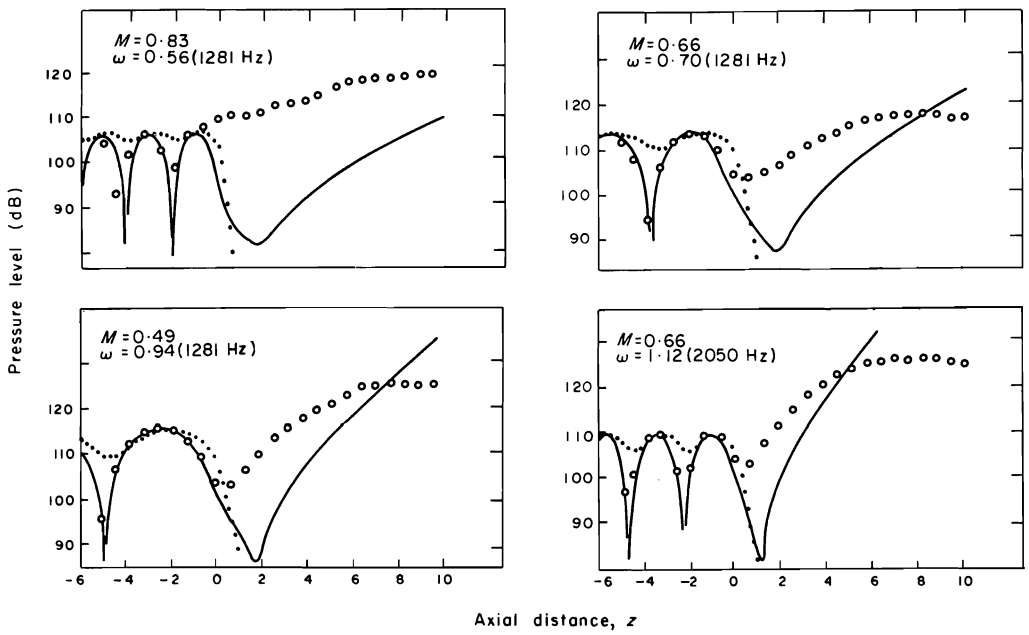

Figure 4. Axial variation of sound pressure level on jet centre-line ($r = 0$). Comparison between experiments (○, Moore's [16] Figure 20) and present analysis (——, Kutta condition, equations (6.5) and (6.6); · · ·, stable, equations (6.1) and (6.2)). Amplitudes are found from the measured maxima in $z < 0$. The outside fields (6.5) and (6.1) are matched to (6.6) and (6.2), respectively, at $z = 0$.

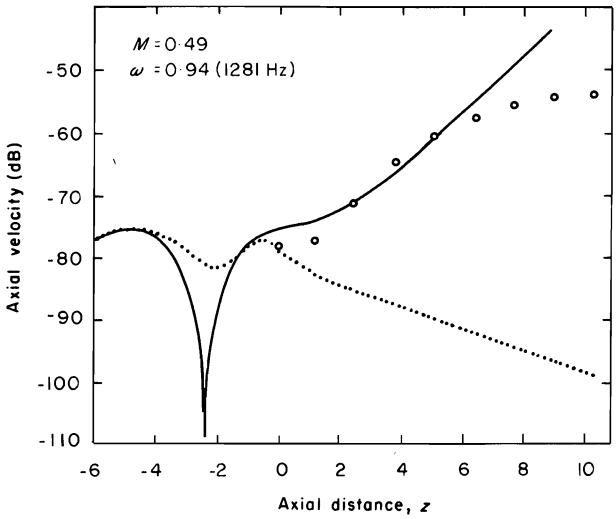

Figure 5. Axial variation of velocity fluctuations ($20 \log_{10} |\frac{1}{2}\sqrt{2} a\phi_z|$) on jet centre-line ($r = 0$). Comparison between experiments (○, Moore's [16] Figure 22) and present analysis (——, Kutta condition, equations (6.7) and (6.8); · · ·, stable, equations (6.3) and (6.4)). Amplitudes are found from the corresponding pressure measurements ($a_k = 2{\cdot}5 \times 10^{-4}$, $a_s = 1{\cdot}25 \times 10^{-4}$). The outside fields (6.7) and (6.3) are matched to (6.8) and (6.4), respectively, at $z = 0$.

TABLE 1

The values of u_0 and u_1 (zeros of $\chi(u)$, equation (4.9)) corresponding to Figures 4 and 5

ω	M	u_0	u_1
0·56	0·83	1·12+0·54i	0·81−0·28i
0·70	0·66	1·35+0·75i	0·91−0·35i
0·94	0·49	1·72+1·17i	1·05−0·44i
1·12	0·66	1·31+1·04i	0·78−0·30i

solution inside the pipe is quite reasonable. In view of the fact that only the Kutta condition gives a reflection coefficient of unity and hence an interference pattern inside the pipe with deep minima, the depth of the measured minima indeed indicates this condition to be appropriate. Also outside the pipe the unstable solution fits the measurements best, although now only qualitatively. An instability wave practically absent in pressure for the first diameters downstream is predicted, but measured is a more upstream starting point. No tendency of improvement for decreasing Strouhal number is showing.

A much better agreement with the instability wave is found for the velocity. For one Strouhal number and Mach number combination a comparison could be made with measured velocity fluctuations. This is shown in Figure 5 (equations (6.3), (6.4), (6.7), (6.8)) and Moore's [16] Figure 22. Since only measurements were available on the jet centre line outside the pipe, the excitation amplitude was taken from the corresponding pressure measurements. The dimensionless amplitude for the Kutta condition solution was found to be $2{\cdot}5 \times 10^{-4}$, and for the stable solution $1{\cdot}25 \times 10^{-4}$. Again, the fields are matched at $z = 0$. Now the Kutta condition solution outside the pipe is clearly seen to agree quite well with the measurements.

From the theory, a purely convective vorticity distribution (i.e., velocity without pressure fluctuations) along the first few diameters of the jet is expected, but this is apparently not found in practice. This discrepancy could be due to the finite Strouhal number, or the actual non-uniform mean velocity profile; however, the few experiments available in this low Strouhal number regime do not permit a conclusive explanation.

7. CONCLUSIONS

A small Strouhal number ω asymptotic analysis has been made of a simple acoustic wave–pipe–jet flow interaction model. The starting point was Munt's [1] acoustically exact formal solution in a form with and without the Kutta condition applied (but with Jones and Morgan's causality condition as adopted by Munt ignored). The velocity and pressure fields inside the pipe and the pressure far field were calculated with a relative error of $O(\omega^2 \ln \omega^{-1})$, while the field in the jet was calculated with a relative error of $O(\omega \ln^{-1/2} \omega^{-1})$. Impedance at the pipe mouth, reflection coefficient upstream inside the pipe, end correction and far field intensity were derived. To quantify the effect of Kutta condition all quantities were calculated for both the stable case (no vortex shedding, pressure singular at the pipe edge) and the Kutta condition case (unstable, pressure finite at the edge).

The Kutta condition affects all the quantities significantly and as a conclusion, at least in the small Strouhal number range, the edge condition must be considered as essential. Therefore, in experiments information on the behaviour near the edge should be sought wherever possible.

The behaviour of the exact solution is shown to be non-uniform for the limit of Helmholtz and Mach number both tending to zero. As an example, the dimensionless end correction may become both 0·6133 for $\omega \to \infty$ and 0·2554 (or indeed some other value for other edge conditions) for $\omega \to 0$. Therefore it seems sensible to present data as function of Strouhal number rather than Helmholtz number in case of small but non-zero Mach number.

Comparison with experiments of the field inside the flow showed, except for a pressure dip immediately downstream the exit, a good agreement.

ACKNOWLEDGMENTS

The problem considered in the present paper was suggested by Professor D. G. Crighton (Leeds). Most of the work is an adapted version of a chapter of the author's thesis, published previously, prepared at and submitted to the Eindhoven Technical University. The first and second supervisor were Professor G. Vossers (Eindhoven) and Professor Crighton, respectively, to whom the author is very grateful for their ever friendly, inspiring and stimulating cooperation. Also he acknowledges the valuable suggestions of Professor J. Boersma (Eindhoven), while the beautiful films of ir. L. J. Poldervaart [28], which provided so much insight into the mechanisms of sound–jet interaction, have to be mentioned. The author is indebted to the University of Leeds for the hospitality it offered the many times he visited it, and to the National Aerospace Laboratory NLR for providing the opportunity to prepare the work for publication.

REFERENCES

1. R. M. MUNT 1977 *Journal of Fluid Mechanics* **83**, 609–640. The interaction of sound with a subsonic jet issuing from a semi-infinite cylindrical pipe.

2. J. W. MILES 1957 *Journal of the Acoustical Society of America* **29**, 226–228. On the reflection of sound at an interface of relative motion.
3. H. S. RIBNER 1957 *Journal of the Acoustical Society of America* **29**, 435–441. Reflection, transmission and amplification of sound by a moving medium.
4. D. G. CRIGHTON and F. G. LEPPINGTON 1974 *Journal of Fluid Mechanics* **64**, 393–414. Radiation properties of the semi-infinite vortex sheet: the initial-value problem.
5. J. D. MORGAN 1974 *Quarterly Journal of Mechanics and Applied Mathematics* **27**, 465–487. The interaction of sound with a semi-infinite vortex sheet.
6. S. D. SAVKAR 1975 *Journal of Sound and Vibration* **42**, 363–386. Radiation of cylindrical duct acoustic modes with flow mismatch.
7. R. M. MUNT (to be submitted) *Journal of Sound and Vibration*. Acoustic transmission properties of a jet pipe with subsonic jet flow, parts I and II.
8. M. S. HOWE 1979 *Journal of Fluid Mechanics* **91**, 209–229. Attenuation of sound in a low Mach number nozzle flow.
9. D. BECHERT 1980 *Journal of Sound and Vibration* **70**, 398–405. Sound absorption caused by vorticity shedding, demonstrated with a jet flow.
10. J. BOERSMA 1978 *Private Communication*.
11. S. W. RIENSTRA 1981 *American Society of Mechanical Engineers Journal of Engineering for Industry* **103**, 378–384 and **104**, 112. On the acoustical implications of vortex shedding from an exhaust pipe.
12. A. M. CARGILL 1979 in *Proceedings of Symposium on Mechanics on Sound Generation in Flows, Göttingen* (editer E.-A. Müller), 19–25. Berlin: Springer-Verlag. Low frequency sound radiation due to the interaction of unsteady flows with a jet pipe.
13. P. MUNGUR and H. E. PLUMBLEE 1979 *American Institute of Aeronautics and Astronautics Paper No.* 79–676. Influence of the jet exhaust flow field on the acoustic radiation impedance of a jet pipe opening.
14. S. C. CROW and F. H. CHAMPAGNE 1971 *Journal of Fluid Mechanics* **48**, 547–591. Orderly structures in jet turbulence.
15. B. H. K. LEE and D. J. JONES 1973 *American Institute of Aeronautics and Astronautics Paper No.* 73–630. Transmission of upstream sound through a subsonic jet.
16. C. J. MOORE 1977 *Journal of Fluid Mechanics* **80**, 321–367. The role of shear-layer instability waves in jet exhaust noise.
17. D. BECHERT, U. MICHEL and E. PFIZENMAIER 1977 *American Institute of Aeronautics and Astronautics Paper No.* 77–1278. Experiments on the transmission of sound through jets.
18. M. J. LIGHTHILL 1960 *Philosophical Transactions of the Royal Society of London, Series A* **252**, 397–430. Studies on magneto-hydrodynamic waves and other anisotropic wave motions.
19. M. E. GOLDSTEIN 1976 *Aeroacoustics*. New York: McGraw-Hill.
20. S. W. RIENSTRA 1981 *Journal of Fluid Mechanics* **108**, 443–460. Sound diffraction at a trailing edge.
21. D. S. JONES and J. D. MORGAN 1972 *Proceedings of the Cambridge Philosophical Society* **72**, 465–488. The instability of a vortex sheet on a subsonic stream under acoustic radiation.
22. S. W. RIENSTRA 1979 *Ph.D. Thesis, Technical University, Eindhoven, Netherlands*. Edge influence on the response of shear layers to acoustic forcing.
23. M. E. GOLDSTEIN 1980 *Journal of Fluid Mechanics* **104**, 217–246. The coupling between flow instabilities and incident disturbances at a leading edge.
24. D. G. CRIGHTON 1981 *Journal of Fluid Mechanics* **106**, 261–298. Acoustics as a branch of fluid mechanics.
25. B. NOBLE 1958 *Methods Based on the Wiener–Hopf Technique*. London: Pergamon Press.
26. G. N. WATSON 1966 *A Treatise on the Theory of Bessel Functions*. Cambridge: University Press, second edition.
27. H. LEVINE and J. SCHWINGER 1948 *Physical Review* **73**, 383–406. On the radiation of sound from an unflanged circular pipe.
28. L. J. POLDERVAART, A. P. J. WIJNANDS and I. BRONKHORST 1974 *Sound Pulse–Boundary Layer Interaction Studies* (film). A. V. Centre, T.H.E., Eindhoven, Netherlands. (Reviewed by J. E. Ffowcs Williams 1976 *Journal of Fluid Mechanics* **78**, 859–862.)